THE JOURNAL OF PHYSICAL CHEMISTRY C

Article

pubs.acs.org/JPCC

Atomic Structure Characterization of Au−Pd Bimetallic Nanoparticles by Aberration-Corrected Scanning Transmission Electron Microscopy

R. Esparza,*[,†] O. Téllez-Vázquez,[†] G. Rodríguez-Ortiz,[†] A. Ángeles-Pascual,[‡] S. Velumani,[‡] and R. Pérez[†]

[†]Centro de Física Aplicada y Tecnología Avanzada, Universidad Nacional Autónoma de México, Boulevard Juriquilla 3001, Santiago de Querétaro, Queretaro 76230, México

[‡]Departamento de Ingeniería Eléctrica-SEES, CINVESTAV-IPN, Av. IPN 2508, Zacatenco, México D.F., 07360, México

ABSTRACT: Au−Pd core−shell nanoparticles were structurally characterized using spherical aberration (Cs) corrected scanning transmission electron microscopy (STEM). The microscope is equipped with a detector of high-angle annular dark field (HAADF)-STEM, in addition with an energy-dispersive X-ray spectrometer (EDS). The high-resolution elemental line-scan was carried out using the combination of STEM-EDS which allowed us to obtain an elemental analysis at atomic level. The effect of the Pd in the formation of Au−Pd core−shell has been studied by HAADF-STEM images and molecular dynamics studies. The obtained results predict that the growth of Pd on the Au core is through the formation of islands, suggesting a preferential growth of the Volmer−Weber type model.

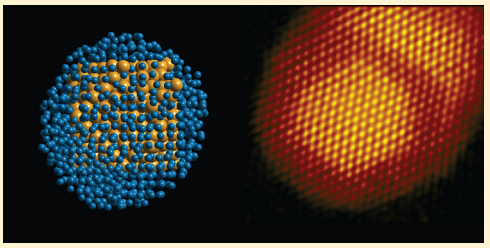

INTRODUCTION

Over the past decade, metal nanoparticles have been the object of new research activities for catalysis.[1] From the catalytic point of view, bimetallic nanoparticles made of two different metal elements have also received considerable attention in the literature, because the bimetallic nanoparticles would make it possible to obtain improved catalytic activity and also create new chemical, physical, and biological properties, which are not obtained with monometallic catalysts. This enhancement in the properties is due to synergistic effects,[2] which originated from the mutual electronic and/or geometrical influence of different neighboring atoms.[3] Among the bimetallic nanoparticles, the gold−palladium (Au−Pd) system has been receiving constant attention in the literature.[4] Recently, it was shown that a combination of Au and Pd in an alloy nanoparticle leads to improved catalytic activity and selectivity in redox processes.[5] Thus, for example, alloying Au and Pd leads to a 25-fold enhancement in activity for the oxidation of phenylethanol.[6] Also, high catalytic performance in hydrogenation reactions is shown by Au−Pd nanoalloys.[7] The enhanced catalytic activity seems to be caused by the modified electronic structure due to high differences in the atomic electron configurations and electronegativities compared to their pure metals.[8]

Bimetallic nanoparticles with controllable structure, composition, size, and morphology can be easily synthesized by different methods such as co-reduction, thermal decomposition, seeded-growth, and galvanic replacement reaction, among others.[9] The successive reduction approach normally gives better control of the morphology and the synthesized Au−Pd bimetallic nanoparticles show core−shell structure.[10] However, the method of synthesis of the Au−Pd bimetallic nanoparticle system with composition, size, and structure in a wide range has not been established. This situation is in part due to the fact that there is the propensity for Pd_2^+ to form precipitates in aqueous solutions when it is used as a precursor in combination with $AuCl_4^-$.[11]

Theoretical simulations based on molecular dynamic methods predict that stable ordered structures of the bimetallic nanoparticle have a Pd core and an Au shell.[12] However, nanoparticles having Au and Pd core−shell can also be formed due to the small difference between the configuration energies. Much of the recent research has been related to the atomic structure determination of the Au−Pd nanoparticles,[13,14] given that this bimetallic system is much more stable than the pure gold and palladium nanoparticles.[6] In this work, the atomic structural characteristics of the Au−Pd core−shell nanoparticles have been obtained using the spherical aberration (Cs) corrected scanning transmission electron microscopy (STEM). Experimental high-angle annular dark field (HAADF)-STEM images have been obtained from the Au−Pd core−shell specimens. Also, theoretical simulations based on molecular dynamics for two different systems have been carried out. In the first system, two gold nanoparticles are allowed to coalesce in a palladium environment. In the second case, two Au−Pd core−shell nanoparticles are allowed to coalesce. At different stages of the coalescent molecular dynamic experiment, the atomic structure of the instant atom arrangement is frozen and used as a possible atomic model for the STEM imaging electron dynamical simulations. Comparisons between the theoretical and experimental STEM images are carried out and some insights from the core−shell atomic structure of the nanoparticles are drawn.

Received: August 1, 2014
Published: August 13, 2014

dx.doi.org/10.1021/jp507794z | J. Phys. Chem. C 2014, 118, 22383−22388

EXPERIMENTAL PROCEDURE

The following chemicals were used as obtained: gold chloride trihydrate ($HAuCl_4$ $3H_2O$), potassium tetrachloropalladate (K_2PdCl_4), sodium borohydride granules ($NaBH_4$), 1.0 M hydrochloric acid solution (HCl), 1.0 M sodium hydroxide solution (NaOH), acetone, hexane, and polyvinylpyrrolidone (PVP) from Sigma-Aldrich. Deionized water with a resistivity of 18.2 MΩ cm was used.

Au nanoparticles were synthesized according to the chemical synthesis method of Eah et al.[15] Briefly, an aqueous solution of 50 mM gold chloride anions ($AuCl_4^-$) in a glass vial was obtained by dissolving $HAuCl_4{\cdot}3H_2O$ with the same molar amount of HCl. Another aqueous solution of 50 mM borohydride anions (BH_4^-) in a glass vial was obtained by dissolving $NaBH_4$ granules with the same molar amount of NaOH. We added 100 μL of the $AuCl_4^-$ solution to a three-necked flask with deionized water and later injected 300 μL of the BH_4^- solution all at once with vigorous stirring. The total weight of the aqueous solution was controlled to be 10 g so that the concentration of gold ions is 0.50 mM. The solution changed color from light yellow to red immediately. A 5.0 g aliquot of acetone was added to the 10 g aqueous solution of gold nanoparticles and stirred for 10 s; inmediately after that 5.0 g of hexane with 0.0025 g of PVP was added, and the flask was stirring vigorously for 30 s. The water−acetone phase became colorless, and the hexane phase turned dark red due to the phase-transfer of gold nanoparticles. No post synthesis cleaning step was employed, since all reaction subproducts remain in the water−acetone phase.

In the second stage, an aqueous solution of 50 mM potassium tetrachloropalladate (K_2PdCl_4) dissolved with the same molar amount of HCl was added to the finished solution of gold nanoparticles and stirring vigorously in a three-necked flask. The solution changed color from a red to brown dark colloidal solution, which confirms the formation of bimetallic nanoparticles.

To characterize the Au−Pd nanoparticles, copper grids with holey carbon film were prepared with a drop of the solution. The samples were analyzed using aberration-corrected (Cs) scanning transmission electron microscopy (STEM) with a Jeol ARM200F (200 kV) FEG-STEM/TEM, equipped with a CEOS Cs corrector on the illumination system. High-angle annular dark field (HAADF)-STEM images were obtained. The probe current used in STEM mode was 23.2 pA (spot size 9C) using a condenser lens aperture size of 40 μm. The HAADF-STEM images were registered using a camera length of 80 mm and a collection angle of 50−180 mrad. Elemental analysis was performed using X-ray energy-dispersive spectroscopy (EDS, Oxford). Images, spectra, and line scans were obtained using the Digital Micrograph software from Gatan.

HAADF-STEM image simulations have been performed using the QSTEM software package[16] which uses the multislice algorithm.[17] The parameters considered for the simulation correspond to the experimental conditions of the microscope.

Molecular dynamics simulations were used to model the growth process of the Au−Pd nanoparticles. In order to simulate this process, the semiempirical analytic embedded-atom method (EAM) was used. Two configurations were explored: the first one, two Au cuboctahedral nanoparticles (561 atoms each) at a distance, one from the other and surrounded with a Pd atoms environment (2060 atoms approximately), and the second one is based in the coalescence of two Au−Pd core−shell nanoparticles (561 atoms each) with an Au nucleus and surrounded with Pd atoms. These approximate models of the nanoparticles were observed in STEM observations.

The simulation was performed based on the canonical ensemble (NVT) using the XenoView program. The time step used to perform the simulation was 0.1 fs (fs). Periodic boundary conditions were applied in all directions of the simulation cell. An Andersen thermostat to maintain constant temperature of the simulation cell at 1100 K was used. The consistent force field (CFF) where the potential energy is calculated as a sum of interatomic potentials was used.

RESULTS AND DISCUSSION

Recently, scanning transmission electron microscopy (STEM) is the technique more widely used in the characterization of monometallic and mostly bimetallic nanoparticles; this is due to high-resolution obtained in STEM microscopes equipped with spherical aberration (Cs) correctors, which reaches resolutions below 0.1 nm (the order of picometers)[18] in addition to the scattered intensity scale which is associated with the atomic number Z of the elements in the sample.[19] The use of metallic particles as core in the synthesis of core−shell structures has been very suitable in many bimetallic systems.[20−22] Figure 1a shows a low-magnification high-angle annular dark-field (HAADF)-STEM image of Au nanoparticles used afterward as core or seed-growth to synthesize the Au−Pd core−shell nanoparticles. The nanoparticles have a homogeneous size distribution with an average particle size of 3.7 nm (size distribution plot inside). The analysis of the structure, size, morphology, and the defects present in the nanoparticles is very important, because they define the final properties of the material. Figure 1b,c shows two high-resolution HAADF-STEM images of gold nanoparticles with a cuboctahedral shape. The Au nanoparticles have some irregular atomic defects on the faceted edge surfaces.

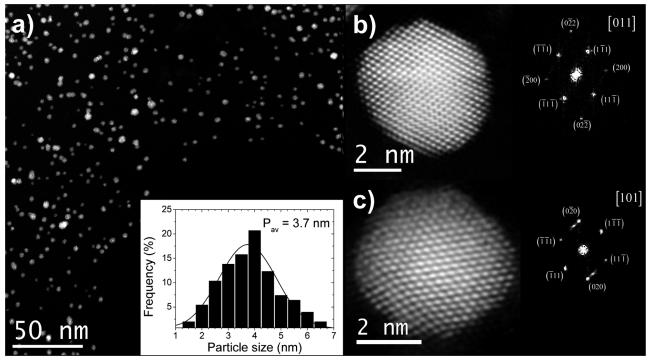

Figure 1. HAADF-STEM images of Au nanoparticles: (a) low-magnification image with size distribution plot inside; (b) and (c) high-resolution HAADF-STEM images of the Au nanoparticles with their corresponding FFT.

In the particular case of Figure 1b, a HAADF-STEM image and its corresponding fast Fourier transform (FFT, beside) d-spacings of 0.2356, 0.2049, and 0.1398 nm were obtained. Such d-spacings correspond to (11−1), (200), and (02−2) crystalline interplanar distances, respectively, of the face-centered cubic (fcc) Au structure with a_0 = 0.4078 nm (JCPDF 04−0784), and the nanoparticle is oriented in the [011] direction. In the case of Figure 1c, d-spacings of 0.2324

dx.doi.org/10.1021/jp507794z | J. Phys. Chem. C 2014, 118, 22383−22388

and 0.2028 nm were obtained which correspond to (11−1) and (020) interplanar distances. respectively. and the nanoparticle is oriented in the [101] direction. As mentioned above, the majority of the synthesized Au nanoparticles had cuboctahedral shapes.

After synthesizing the Au nanoparticles, they were used as core and coated by Pd atoms, thus obtaining Au−Pd core−shell nanoparticles. Figure 2a shows a low-magnification HAADF-STEM image of Au−Pd nanoparticles. As can be observed, the bimetallic nanoparticles have a homogeneous size distribution with an average particle size of 5.5 nm (size distribution plot inside). The average particle size is higher than that of monometallic Au nanoparticles, due to incorporation of the Pd atoms on the surface of the nanoparticles. Figure 2b shows an energy-dispersive X-ray (EDS) spectrum of the elemental composition of the nanoparticles. The spectrum shows the presence of Au and Pd, which indicate the incorporation of Pd in the solution. Figure 2c shows polycrystalline selected area electron diffraction (SAED) pattern obtained from the bimetallic nanoparticles, in which the mixed diffraction rings correspond to the face-centered cubic (fcc) structure of the Au and Pd, with reticular parameters a_0 = 0.4078 nm and a_0 = 0.3890 nm, respectively. However, the analysis of the polycrystalline SAED pattern cannot indicate if the bimetallic nanoparticles have a core−shell structure or they are only single Au and Pd mixed nanoparticles.

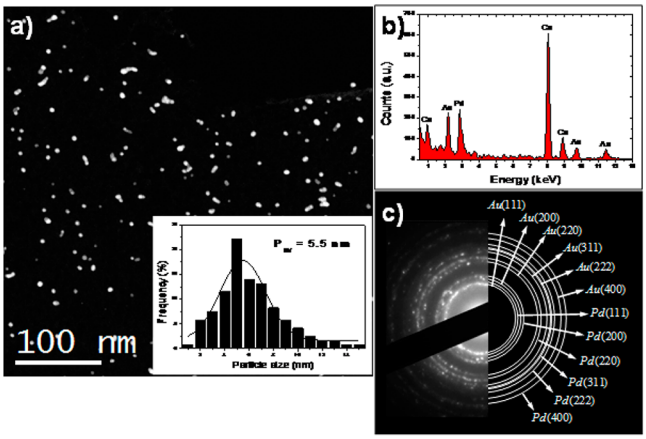

Figure 2. (a) HAADF-STEM image of Au−Pd nanoparticles with particle size distribution plot. (b) EDS spectrum shows the presence of Au and Pd in the elemental composition of the nanoparticles. (c) SAED pattern.

The physical properties of the nanoparticles are associated with their particle size, structure, morphology, and also their chemical composition. STEM combined with EDS is one of the most widely used techniques for performing microanalysis of the bimetallic nanoparticles.[20] The analysis of the composition and distribution of the elements Au and Pd in the nanoparticles was obtained using this technique. Figure 3a shows a HAADF-STEM image of a nanoparticle Au−Pd core−shell indicating the region of elemental analysis. As can be observed, the nanoparticle has a variation in contrast which is associated with the atomic number of the elements, the strong brightness contrast corresponding to Au atomic sites while low brightness contrast corresponds to Pd atoms. Figure 3b shows the STEM-EDS line-scan across the nanoparticle Au−Pd core−shell. The Au-L and the Pd-L signals were traced across the region of individual Au and Pd layers with the maximum intensity of the signals. From the signals, varying intensity can be clearly seen along the different regions of the nanoparticles. The line-scan profile on the particle shows strong Pd signals at the particle edge and strong Au signals in the particle center, revealing a typical core−shell structure. Both techniques in STEM, image and analysis, confirm that the nanoparticles have a core−shell structure. Almost all the bimetallic nanoparticles obtained with the described synthesis method have a core−shell structure. However, some aggregates of Au−Pd core−shell were formed, which will be discussed later in further detail.

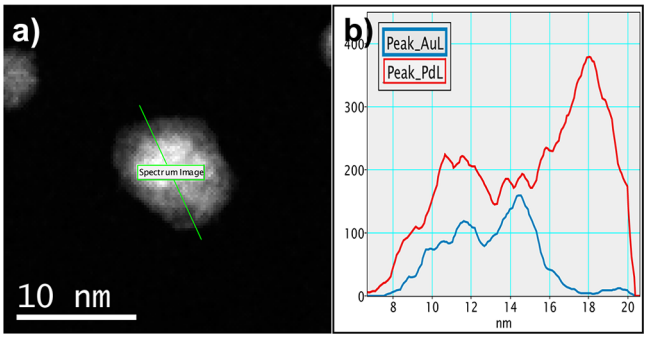

Figure 3. STEM-EDS elemental analysis by line-scan across the nanoparticle Au−Pd core−shell: (a) HAADF-STEM image of the corresponding Au−Pd core−shell nanoparticle; (b) elemental line-scan indicating the presence of Au in the core and Pd in the shell.

The intensity of the HAADF-STEM images is directly proportional to the density and thickness of the specimen and proportional to $Z^{3/2}$, where Z is the atomic number of the sample.[23] Therefore, the brightness contrast of the Au atoms appears more intense than that of the Pd atoms, as shown in the previous figure. As has been mentioned, almost all the nanoparticles have a core−shell structure; however, some nanoparticles form aggregates. These aggregates have the same structure as the original nanoparticles, that is, core−shell structure. Figure 4a shows a HAADF-STEM image of aggregated Au−Pd core−shell nanoparticles. As can be observed, in all the nanoparticles the core−shell structure was maintained. Figure 4b shows an image from an Au−Pd core−shell nanoparticle with three gold regions surrounded by a layer of Pd atoms and also with Pd neck regions. The diffusion of Au atoms from the Au core region is clearly illustrated. Figure 4c shows a high-resolution HAADF-STEM image of an Au−Pd core−shell nanoparticle. The morphology of this nanoparticle corresponds to a cuboctahedron. From the image, the two differences in contrast caused by atomic composition of the nanoparticle are clearly evident. The diameter of the nanoparticles is about 6.5 nm. This consists of an Au core (3.5 nm) and a Pd rich outer shell (3 nm) as can be seen from the contrasts in the HAADF-STEM image. In addition, a third semilayer is observed, which consists of Au atoms. Figure 4d shows the FFT obtained from the HAADF-STEM image, where the measurement of the spots is associated with the lattice planes of the fcc-Au and fcc-Pd structures, and furthermore, the incident electron beam direction is along [011]. From the spots identified with blue squares *d*-spacings of 0.2326, 0.2341, and 0.2051 nm were obtained, which correspond to (111), (111), and (200) lattice planes of Au (JCPDF 04−0784), and from the spots identified with red circle *d*-spacings of 0.2284, 0.2278, and 0.1956 nm were obtained, which correspond to (111), (111), and (200) lattice planes of Pd (JCPDF 05−0681).

dx.doi.org/10.1021/jp507794z | J. Phys. Chem. C 2014, 118, 22383−22388

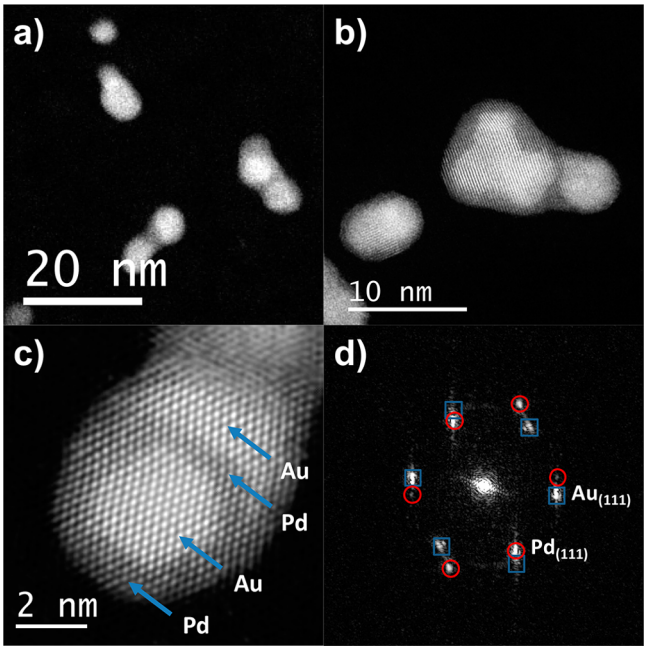

Figure 4. (a,b) HAADF-STEM images showing some aggregated Au–Pd core–shell nanoparticles. (c) High-resolution HAADF-STEM image showing an Au–Pd core–shell nanoparticle. (d) FFT shows the corresponding lattice indexing of the Au and Pd.

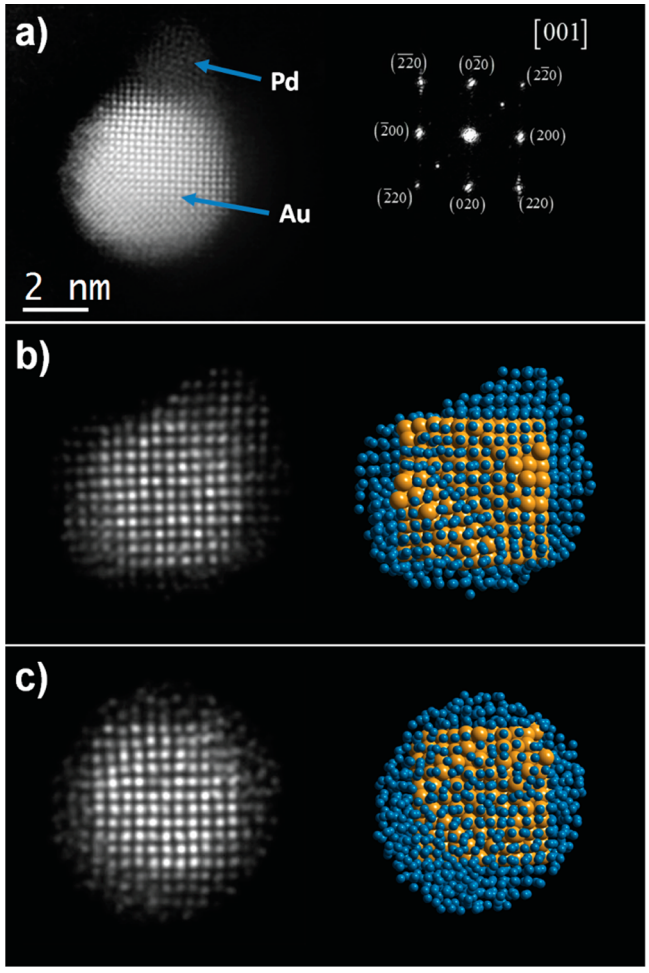

Figure 5. (a) HAADF-STEM image of Au nanoparticle with segregated Pd atoms. (b,c) Simulated HAADF-STEM images with their corresponding atomic model.

The seeded-growth approach provides a very effective method for generating bimetallic nanoparticles with well-controlled nanostructures, core–shell and heterostructured bimetallic compounds, which are especially easy to prepare.[24] When the secondary metal is uniformly deposited on the surface of the preformed seed, core–shell nanostructures will be obtained, while heterostructured nanoparticles can be synthesized if the deposition and growth of the second metal occur on a specific site on the seed.[25] Generally, in order to obtain bimetallic nanostructures based on the seeded-growth process, heterogeneous nucleation and simple growth via atomic addition must be achieved and homogeneous nucleation should be avoided.[26] In the particular case of the Au–Pd bimetallic nanoparticles synthesized in this work, the nanoparticles have a heterogeneous nucleation, in which the Pd atoms are deposited on specific sites of the Au nanoparticles. Figure 5a shows a high-resolution HAADF-STEM image of a nanoparticle where the Pd atoms have a heteroepitaxial growth on the Au nanoparticle. This type of growth mode is the so-called Volmer–Weber (VW) or island growth mode, where the deposited metal grows on high energy sites of substrate metal particle to form islands in order to minimize strain energy.[27] From the image (Figure 5a) and its corresponding FFT (beside) *d*-spacings of 0.2038, 0.2035, and 0.1447 nm were obtained, which correspond to (200), (020), and (220) lattice planes of Au (JCPDF 04–0784) and the incident electron beam direction is along [001]. As mentioned, the Pd atoms grow on the surface of the Au nanoparticle in island growth mode. This behavior generates more islands formed on different sites of the nanoparticle. Figure 5b shows a simulated HAADF-STEM image and its corresponding atomic model beside it, obtained from the molecular dynamic simulations where at the beginning of the simulation process, one Au cuboctahedral nanoparticle was surrounded by a Pd atom environment. From the simulated image and the atomic model, it is clearly evident that the Pd atoms are deposited on the surface of the Au nanoparticle and they grow forming islands, similar to what was observed in the image of Figure 5a. The simulation process continues, and thus the Pd islands continue growing until they completely surrounded the Au nanoparticle, forming the core–shell structure, as can be seen in Figure 5c, where the simulated HAADF-STEM and atomic model are illustrated.

During the synthesis of the Au–Pd bimetallic nanoparticles, many different morphological shapes can be obtained. Two of the more common structures obtained in this work are the single Au–Pd core–shell nanoparticle with an Au nucleus and the other, the aggregated Au–Pd nanoparticles with two and sometimes three Au nuclei. Insights on the formation mechanisms of these morphologies can be explored using molecular dynamic simulations. During the evolution, instant atomic structures of the system are obtained and subsequently used as the supercell for the HAADF-STEM electron diffraction simulations.

As possible examples, two different initial structural conditions are explored. In the first case, the system is based on two Au cuboctahedral nanoparticles a few nanometers apart, and surrounded by a Pd atom environment (Figure 6a). This system is allowed for a dynamical evolution. Figure 6a–d shows the partial evolution of the obtained structures of this system,

dx.doi.org/10.1021/jp507794z | J. Phys. Chem. C 2014, 118, 22383–22388

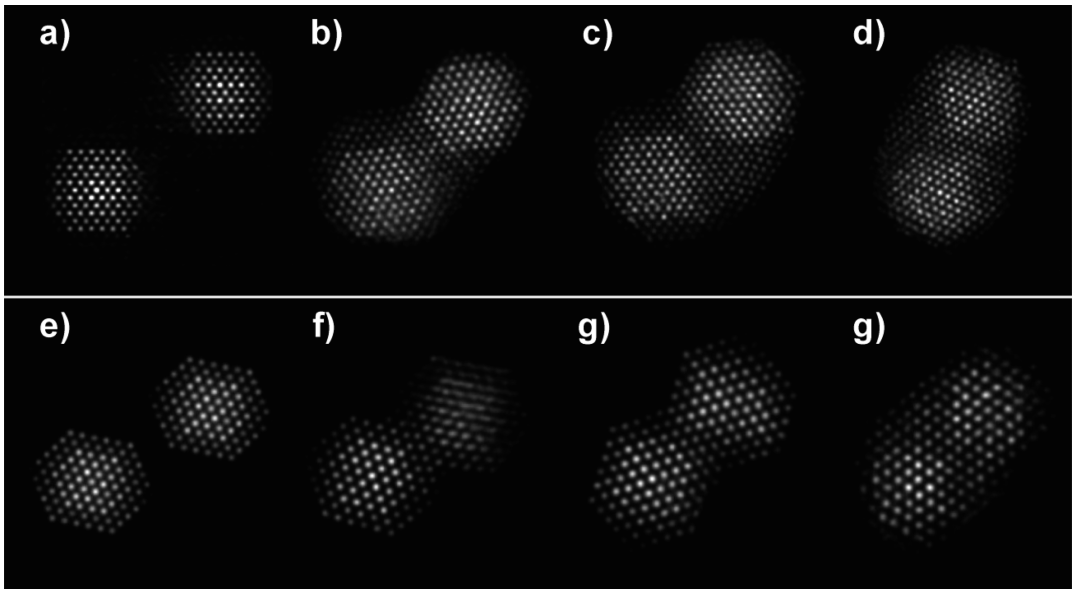

Figure 6. Theoretical HAADF-STEM images obtained from frozen structures of a molecular dynamic coalescence experiment: (a–d) Au cuboctahedral nanoparticles surrounded with a Pd atoms environment and (e–g) coalescence of two Au–Pd core–shell nanoparticles.

which are illustrated from the simulated HAADF-STEM images. After some evolution time, the nanoparticles are found surrounded by a Pd layer and a clear Pd neck is formed (Figure 6b). Figure 6c shows the diffusion of the Pd atoms to the neck region and finally Figure 6d shows the formation of two Au nuclei surrounded by Pd atoms. The second initial structural case is based on the coalescence of two Au–Pd core–shell nanoparticles with an Au nucleus surrounded by Pd atoms (Figure 6e). Figure 6e–g shows the simulated HAADF-STEM images obtained from the frozen atomic structures of the coalescence experiment. Figure 6f shows the two Au nuclei with the clear formation of a Pd neck region. Figure 6g shows the Au atomic diffusion from the Au nanoparticles to the Pd region, and the Pd neck region is larger. Finally, Figure 6h shows the coalescence of the two Au–Pd core–shell nanoparticles with the formation of two Au nuclei surrounded by Pd atoms. As can be observed, Figure 6d and g are similar, which is the result of two different evolutions of Au–Pd system configurations. In both cases, the neck formation by the Pd atoms, the Au atomic diffusion from the nanoparticles to the neck region, and the tendency to formation of two Au nuclei can be obtained. However, it is very important to know which bimetallic system is more stable.

In order to determine the stability conditions of the Au cuboctahedral nanoparticles surrounded with a Pd atom environment and the coalescence of two Au–Pd core–shell nanoparticles, molecular dynamics simulations using a heating process from 300 to 1500 K were carried out. Figure 7 shows the plot of the potential energy per atom with respect to temperature; in addition, the two initial models of the configurations are shown. The temperature was increased linearly by heating at the rate of 5×10^{-3} K/s. As a result, the potential energies at different temperatures were determined for the two configurations. It can be seen in both cases that the behavior of the potential energy per atom is almost similar; however, when the simulation process finished, the configuration of Au cuboctahedral nanoparticles surrounded by Pd atoms has a lower energy per atom than the configuration where two Au–Pd core–shell nanoparticles coalesce; therefore,

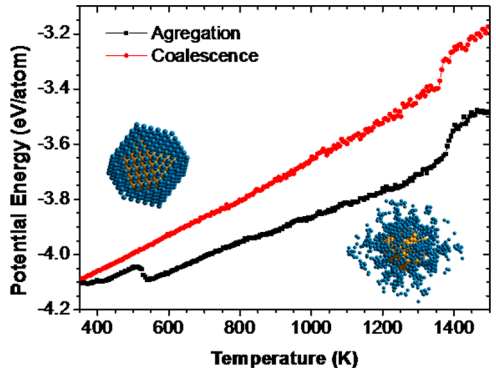

Figure 7. Variation of the energy per atom with respect to the temperature of the two explored configurations.

the first system is more stable after the heating process. The jump in the potential energy of both configurations is the result of the latent heat of fusion released upon melting. For palladium nanoparticles with diameters of 3 or 5 nm, melting temperatures of 1400 and 1600 K, respectively, have been reported, which are consistent with the data obtained in our simulation.[28] Finally, at the end of the heating process, the atomic configuration of Au cuboctahedral nanoparticles surrounded by Pd atoms is almost similar to that observed experimentally by HAADF-STEM, indicating that energetically it is more probable that the Pd atoms have preferential growth on the Au nanoparticles.

CONCLUSIONS

A novel methodology for the atomic structure characterization of Au–Pd core–shell nanoparticles has been shown. In this case, characterization of the bimetallic core–shell nanoparticles was carried out by Cs-corrected STEM. The morphology of the nanoparticles has been studied by a high-resolution HAADF-STEM technique that showed Au particles with preferential surfaces enriched with Pd atoms. The synthesis method used in the preparation of the bimetallic core–shell nanoparticles is surface reduction of the Pd atoms on preformed Au core seeds,

dx.doi.org/10.1021/jp507794z | J. Phys. Chem. C 2014, 118, 22383–22388

by which particles with an average size of 5.5 nm were obtained. The contrast of the HAADF-STEM images showed a high brightness contrast in the core corresponding to Au and low brightness contrast in the shell corresponding to Pd, which was verified by line-scan elemental composition using STEM-EDS; this confirms the Au−Pd core−shell structure. Molecular dynamics simulations were carried out to systematically investigate the structural and thermal stabilities of two structural conditions proposed: Au cuboctahedral nanoparticles surrounded with a Pd atom environment and the other, the coalescence of two Au−Pd core−shell nanoparticles. The results showed that the Au cuboctahedral nanoparticles surrounded by a Pd atom environment had better structural stability, suggesting preferential growth of a Volmer−Weber type model. Our results make it possible to realize an outstanding atomic characterization of the bimetallic core−shell nanoparticles by using Cs-corrected HAADF-STEM, simulations of HAADF-STEM images and molecular dynamics simulations, which is advisible for the knowledge of the selectivity of catalysts for many chemical reactions.

AUTHOR INFORMATION

Corresponding Author

*E-mail: resparza@fata.unam.mx; Phone: +52 (55) 5623-4150.

Author Contributions

The manuscript was written through contributions of all authors. All authors have given approval to the final version of the manuscript.

Notes

The authors declare no competing financial interest.

ACKNOWLEDGMENTS

The authors would like to acknowledge to the PAPIIT-DGAPA for financial support with grant IN110113. Also, the authors acknowledge the Laboratorio Avanzado de Nanoscopia Electrónica "LANE" at the CINVESTAV-Zacatenco.

REFERENCES

(1) Astruc, D.; Lu, F.; Ruiz-Aranzaes, J. Nanoparticles as Recyclable Catalysts: The Frontier between Homogeneous and Heterogeneous Catalysis. *Angew. Chem., Int. Ed.* **2005**, *44*, 7852−7872.

(2) Habas, S. E.; Lee, H.; Radmilovic, V.; Somorjai, G. A.; Yang, P. Shaping Binary Metal Nanocrystals through Epitaxial Seeded Growth. *Nat. Mater.* **2007**, *6*, 692−697.

(3) Yu, W. T.; Porosoff, M. D.; Chen, J. G. Review of Pt-Based Bimetallic Catalysis: From Model Surfaces to Supported Catalysts. *Chem. Rev.* **2012**, *112*, 5780−5817.

(4) Evangelisti, C.; Schiavi, E.; Aronica, L. A.; Caporusso, A. M.; Vitulli, G.; Bertinetti, L.; Martra, G.; Balerna, A.; Mobilio, S. Bimetallic Gold−Palladium Vapour Derived Catalysts: The Role of Structural Features on Their Catalytic Activity. *J. Catal.* **2012**, *286*, 224−236.

(5) Dimitratos, N.; Lopez-Sanchez, J. A.; Anthonykutty, J. M.; Brett, G.; Carley, A. F.; Tiruvalam, R. C.; Herzing, A. A.; Kiely, C. J.; Knight, D. W.; Hutchings, G. J. Oxidation of Glycerol Using Gold−Palladium Alloy-supported Nanocrystals. *Phys. Chem. Chem. Phys.* **2009**, *11*, 4952−4961.

(6) Enache, D. I.; Edwards, J. K.; Landon, P.; Solsona-Espriu, B.; Carley, A. F.; Herzing, A. A.; Watanabe, M.; Kiely, C. J.; Knight, D. W.; Hutchings, G. J. Solvent-Free Oxidation of Primary Alcohols to Aldehydes Using Au-Pd/TiO_2. *Catal. Sci.* **2006**, *311*, 362−365.

(7) Bonnemann, H.; Endruschat, U.; Tesche, B.; Rufinska, A.; Lehmann, C. W.; Wagner, F. E.; Filoti, G.; Parvulescu, V.; Parvulescu, V. I. An SiO_2-embedded Nanoscopic Pd/Au Alloy Colloid. *Eur. J. Inorg. Chem.* **2000**, *5*, 819−822.

(8) Ferrando, R.; Jellinek, J.; Johnston, R. L. Nanoalloys: From Theory to Applications of Alloy Clusters and Nanoparticles. *Chem. Rev.* **2008**, *108*, 845−910.

(9) Wang, D.; Li, Y. Bimetallic Nanocrystals: Liquid-Phase Synthesis and Catalytic Applications. *Adv. Mater.* **2011**, *23*, 1044−1060.

(10) Ferrer, D.; Torres-Castro, A.; Gao, X.; Sepulveda-Guzman, S.; Ortiz-Mendez, U.; Jose-Yacaman, M. Three-Layer Core/Shell Structure in Au−Pd Bimetallic Nanoparticles. *Nano Lett.* **2007**, *7*, 1701−1705.

(11) Venkatesan, P.; Santhanalakshmi, J. Core-Shell Bimetallic Au-Pd Nanoparticles: Synthesis, Structure, Optical and Catalytic Properties. *Nanosci. Nanotechnol.* **2011**, *1*, 43−47.

(12) Liu, H. B.; Pal, U.; Medina, A.; Maldonado, C.; Ascencio, J. A. Structural Incoherency and Structure Reversal in Bimetallic Au - Pd Nanoclusters. *Phys. Rev. B* **2005**, *71*, 075403.

(13) Mayoral, A.; Deepak, F. L.; Esparza, R.; Casillas, G.; Magen, C.; Perez-Tijerina, E.; Jose-Yacaman, M. On the Structure of Bimetallic Noble Metal nanoparticles as Revealed by Aberration Corrected Scanning Transmission Electron Microscopy (STEM). *Micron* **2012**, *43*, 557−564.

(14) Deepak, F. L.; Casillas-Garcia, G.; Esparza, R.; Barron, H.; Jose-Yacaman, M. New Insights into the Structure of PdAu Nanoparticles as Revealed by Aberration-corrected STEM. *J. Cryst. Growth* **2011**, *325*, 60−67.

(15) Martin, M. N.; Basham, J. I.; Chando, P.; Eah, S.-K. Charged Gold Nanoparticles in Non-Polar Solvents: 10-min Synthesis and 2D Self-Assembly. *Langmuir* **2010**, *26*, 7410−7417.

(16) Koch, C. *Determination of Core Structure Periodicity and Point Defect Density along Dislocations*; Arizona State University, Pheonix, Arizona, 2002.

(17) Cowley, J. M.; Moodie, A. F. The Scattering of Electrons by Atoms and Crystals. I. A New Theoretical Approach. *Acta Crystallogr.* **1957**, *10*, 609−619.

(18) Mayoral, A.; Esparza, R.; Deepak, F. L.; Casillas, G.; Mejía-Rosales, S.; Ponce, A.; José-Yacamán, M. Study of Nanoparticles at UTSA: One Year of Using the First ARM-200F Installed in USA. *JEOL News* **2011**, *46*, 1−5.

(19) Erni, R. *Aberration-Corrected Imaging in Transmission Electron Microscopy - An Introduction*; Imperial College Press: London, 2010.

(20) Esparza, R.; García-Ruiz, A. F.; Velázquez Salazar, J. J.; Pérez, R.; José-Yacamán, M. Structural Characterization of Pt−Pd Core−Shell Nanoparticles by Cs-corrected STEM. *J. Nanopart. Res.* **2013**, *15*, 1342.

(21) Chaudhuri, R. G.; Paria, S. Core/Shell Nanoparticles: Classes, Properties, Synthesis Mechanisms, Characterization, and Applications. *Chem. Rev.* **2012**, *112*, 2373−2433.

(22) Cho, S. J.; Ryoo, R. Design of Bimetallic Nanoparticles. *Int. J. Nanotechnol.* **2006**, *3*, 194−215.

(23) Nellist, P. D.; Pennycook, S. J. The Principles and Interpretation of Annular Dark-field Z-Contrast Imaging. *Adv. Imag. Electr. Phys.* **2000**, *113*, 147−203.

(24) Peng, Z.; Wu, J.; Yang, H. Synthesis and Oxygen Reduction Electrocatalytic Property of Platinum Hollow and Platinum-on-Silver Nanoparticles. *Chem. Mater.* **2010**, *22*, 1098−1106.

(25) Peng, X. Mechanisms for the Shape-Control and Shape-Evolution of Colloidal Semiconductor Nanocrystals. *Adv. Mater.* **2003**, *15*, 459−463.

(26) Zeng, J.; Huang, J.; Liu, C.; Wu, C. H.; Lin, Y.; Wang, X.; Zhang, S.; Hou, J.; Xia, Y. Gold-Based Hybrid Nanocrystals Through Heterogeneous Nucleation and Growth. *Adv. Mater.* **2010**, *22*, 1936−1940.

(27) Sitter, H.; Resel, R.; Koller, G.; Ramsey, M. G.; Andreev, A.; Teichert, C. *Fundamentals of Organic Film Growth and Characterisation. In Organic Nanostructures for Next Generation Devices*; Al-Shamery, K. H., Rubahn, H.-G., Sitter, H., Eds.; Springer-Verlag: Berlin, 2008; Chapter 1, pp 3−20.

(28) Grammatikopoulos, P.; Cassidy, C.; Singh, V.; Sowwan, M. Coalescence-induced Crystallization Wave in Pd Nanoparticles. *Nat. Sci. Rep.* **2014**, *4*, 1−9.